A unipolar nano-diode detector with improved performance using high-k material SiN_x

DOI:
10.1088/1361-6641/aae2f5

Document Version
Accepted author manuscript

Published in:
Semiconductor Science and Technology

IOP Publishing Journal Title
Journal **XX** (XXXX) XXXXXX https://doi.org/XXXX/XXXX

Unipolar nano-diode detector with improved performance using high-k material SiN_x

Linqing Zhang [1], Haiping Zhou [2], Jiawei Zhang[1], Qingpu Wang[3], Yifei Zhang[3] and Aimin Song[1, 3, 4]

[1] School of Electrical and Electronic Engineering, University of Manchester, Manchester, United Kingdom
[2] School of Engineering, University of Glasgow, Glasgow, United Kingdom
[3] The Center of Nanoelectronics and School of Microelectronics, Shandong University, Jinan, China
[4] The State Key Laboratory of Crystal Materials, Shandong University, Jinan, China

E-mail: yifeizhang@sdu.edu.cn, A.Song@manchester.ac.uk

Abstract

The performance of a solid-state planar nano-diode, namely self-switching diode (SSD), is improved by depositing a 100-nm-thick SiN_x film with high dielectric constant (high-k) into the insulating nano-trenches. The SiN_x film grown by using plasma-enhanced chemical vapour deposition (PECVD) can enhance the electric field coupling over the trenches and thus increase the accumulated charges for field effect. In this case, the current-voltage nonlinearity is improved significantly and the responsivity of high frequency rectification is also increased by a factor of almost one order up to 100 GHz. In addition, compared to the device without SiN_x coating, the low frequency noise of the proposed diode is suppressed dramatically. The improved responsivity and noise-equivalent power (NEP) of 11 SSDs in parallel with SiN_x coating are 110 V/W at 50 GHz and 180 $pW/Hz^{1/2}$, which are comparable to the state-of-the-art data of reported SSD arrays.

Keywords: Self-switching diode, SiN_x, High-k, Nano rectifier

1. Introduction

Terahertz technologies have been envisaged to have promising applications in medical and security imaging, pharmaceutical compound analysis, and radio astronomy etc. [1]. However, the frequency band is often called 'terahertz gap' due to a lack of high performance solid-state terahertz detectors and emitters at room temperature. Among the reported novel detectors [2, 3], a nano-scale self-switching diode (SSD) is a promising candidate for real applications. An SSD based on GaAs/AlGaAs heterostructure containing a two-dimensional electron gas (2DEG) has been shown to operate at frequencies up to 1.5 THz without any DC bias at room temperature [4]. Successful detection of free-space terahertz radiation between 1.3 and 2.5 THz at low temperatures from 10 to 150 K has also been demonstrated by SSDs fabricated using an InGaAs/InP 2DEG wafer [5]. In addition, SSDs have been realized using other semiconductor materials, such as InAs/AlAs [6], GaN/AlGaN [7] and 2D materials [8]. For terahertz detectors, responsivity and noise performance are two most important factors. By connecting about 2000 SSDs in parallel, the thermal noise of the SSD array was significantly reduced and the noise-equivalent power (NEP) was improved to a value of 64 $pW/Hz^{1/2}$ [9], among the lowest ones of the reported terahertz detectors.

Additionally, modelling and simulation of SSD have been carried out intensively [10-13]. A number of simulations predicted that the SSD performance can be improved significantly if its nano-trenches are filled with high-k materials [14-17]. However, to the best of our knowledge, no fabricated device has been reported to demonstrate this yet. On the other hand, high-k materials have already been widely used as a substitute for SiO_2 in electronics to achieve high mobility, low threshold voltage and low leakage [18-21]. Examples are HfO_2 [22], Si_3N_4 [23], SiO_xN_y [24] and

HfSiON [25]. In this work, SSD arrays are fabricated on 2DEG $In_{53}Ga_{47}As$ substrate with high-k SiN_x filling for their nano-trenches, achieving high responsivity and low noise. Such improvement is highly desired for terahertz detection at room temperature.

2. Experiment

An InGaAs/InAlAs 2DEG wafer from IQE Inc. was used to fabricate the SSDs. The 2DEG embedded in the InGaAs/InAlAs heterostructure is located 25 nm below the surface, as depicted in Figure 1(a). The carrier density and electron mobility of the 2DEG are 1.3×10^{12} cm^{-2} and 10,400 $cm^2/V\cdot s$ at 300 K, respectively. The relatively high electron mobility of the InGaAs/InAlAs based 2DEGs is beneficial for high frequency detection. The active area of the diode, consisting of asymmetric nanochannels defined with nano-trenches, was fabricated using electron-beam lithography, as shown in Figure 1(b). The SSD structure was then transferred into the substrate by bromine-based wet etching, which stops at the InAlAs buffer layer. The depth of the insulation trench is around 50 nm measured by atomic force microscopy (AFM), and the width is about 150 nm. The trenches can force the electrons to flow only through the nanochannels.

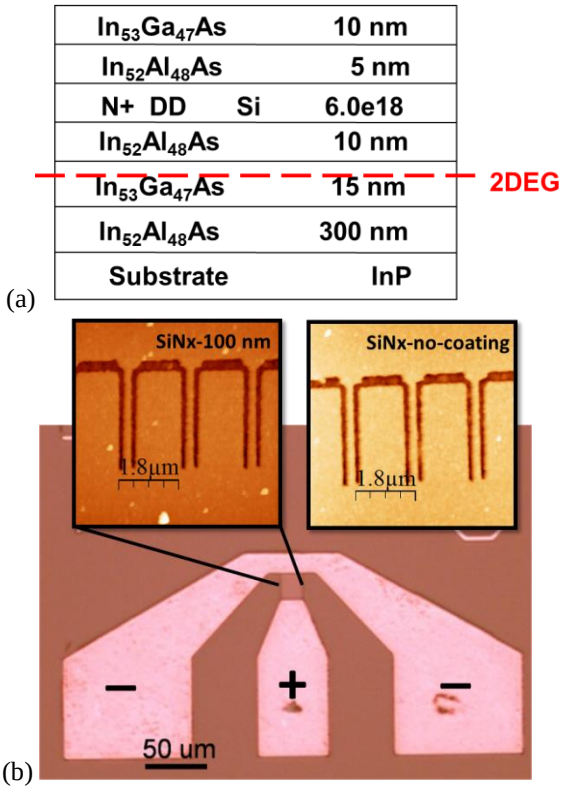

Figure 1. (a) Structure of InGaAs/InAlAs 2DEG wafer. (b) AFM images of the etched SSD array with and without SiN_x coating with co-planar waveguide ohmic contacts. The SSD channel is 3 μm long and 215 nm wide.

With the device unbiased, the effective channel is actually narrower than the geometric width due to the depletion region at the etched boundaries, which is introduced by the charges of surface states. The amount of surface charges could be affected by surface roughness, charge states, Fermi-level pinning and surface treatments [26]. The effective channel of the SSD can be widened or narrowed with forward or reverse bias respectively. This corresponds to the nonlinearity and thus a high-frequency rectification.

11 SSDs are accommodated in parallel on a mesa structure, as shown in Figure 1(b), which are fed by using a co-planar waveguide (CPW) with an impedance of 50 Ω for rectification characterisation. The signal and gap width of the CPW is 60 μm and 55 μm, respectively. To reduce the ohmic contact resistance, the electrodes are fabricated with Au/Ge/Ni/Au. The measured ohmic contact resistance is 0.86 Ω.mm and the specific resistance is 4×10^{-5} $\Omega.cm^2$.

SiN_x has been widely used as passivation for electronic devices, such as the field effect transistor (FET) [27] and high-electron-mobility transistor (HEMT) [28]. To improve the performance of the SSDs, the SiN_x coating was grown by plasma-enhanced chemical vapour deposition (PECVD), which offers excellent dielectric properties of the deposited and conformed step coverage [29]. The deposition was carried out with SiH_4, NH_3 and N_2 at flow rates of 10, 16, 170 sccm, respectively, at 300 ^oC. The thickness of the SiN_x coating was 100 nm, namely twice that of the trench depth, so that the trenches were completely filled. The proposed device is nominated as 'SiN_x-100 nm' while another device without coating is nominated 'SiN_x-no-coating'. These will be used for comparison in the following sections.

3. Results and discussion

3.1 I-V Characterisation

The devices were characterised at room temperature in the dark, by using Agilent E5270B semiconductor analyser. As the positive forward bias was increased, the current first increased rapidly and then quasi-linearly due to the series resistance, as shown in Figure 2(a). With a negative bias, the reverse current exists as the channel is not completely pinched off. Compared to that of the uncoated device, both the forward and reverse currents of the coated device are clearly increased, as shown in Figure 2(a). This is as expected from the enhanced field coupling over the trenches and the reduced electric field strength on the channel. However, note that the device nonlinearity, given by *[I(V)+I(-V)]/2*, is significantly enhanced particularly at low bias values, which are conditions desired for high-frequency rectification, as plotted in Figure 2(b). For instance, the nonlinearity of the current-voltage (I-V) curve is enhanced by a factor of about 18 at 0.1 V.

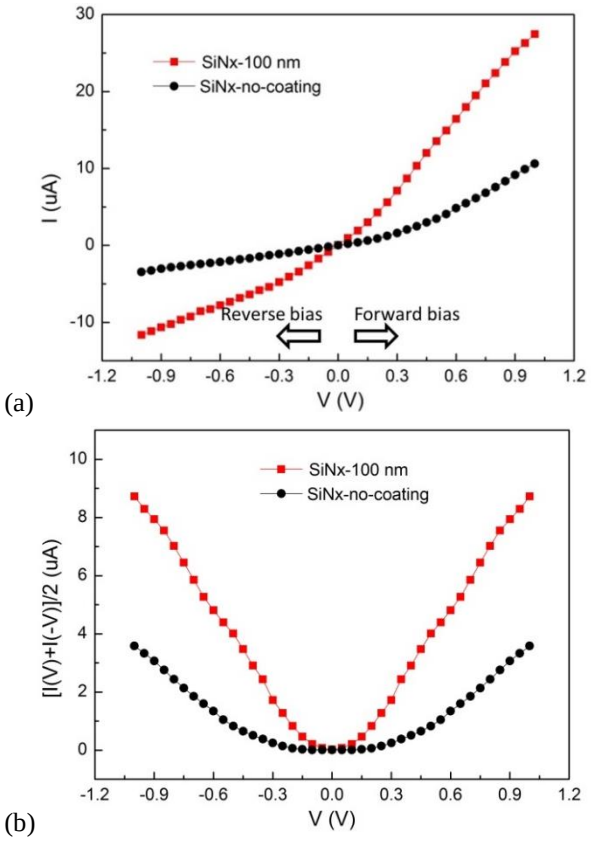

Figure 2. (a) The I-V characteristics of SiN_x-100 nm and SiN_x-no-coating. (b) The extracted nonlinear component of the I-V curves in (a).

3.2 RF Characterisation

An Agilent 8510XF vector network analyser (VNA) providing continuous frequency coverage from 45 MHz to 100 GHz was employed for high-frequency rectification measurement. The DC bias was provided with Keithley 2400 source measure unit through a bias-T, and the input power was calibrated before being fed into SSDs device. Figure 3(a) illustrates the rectified output voltages of the devices at zero bias. It can be seen that the output voltage of the device with SiN_x coating is clearly higher than that of its uncoated counterpart, which reveals the strong enhancement of the responsivity. Figure 3(b) shows the output voltage as a function of input power measured at 50 GHz and zero bias. The output voltage is proportional to the input power, which corresponds to the square-law operation of the device. The extrinsic responsivity of the devices can be calculated by dividing the measured output voltage by the input power (-5.5 dBm). The extrinsic responsivity of the device SiN_x-100 nm is 110 V/W at 50 GHz, which is much higher than that of SiN_x-no-coating, 6.99 V/W. By integrating thousands of SSDs with high-k coating in parallel, the input impedance can further reduce from 33.3 kΩ (the zero-bias resistance) down to hundreds of ohms for better impedance matching and noise performance [9].

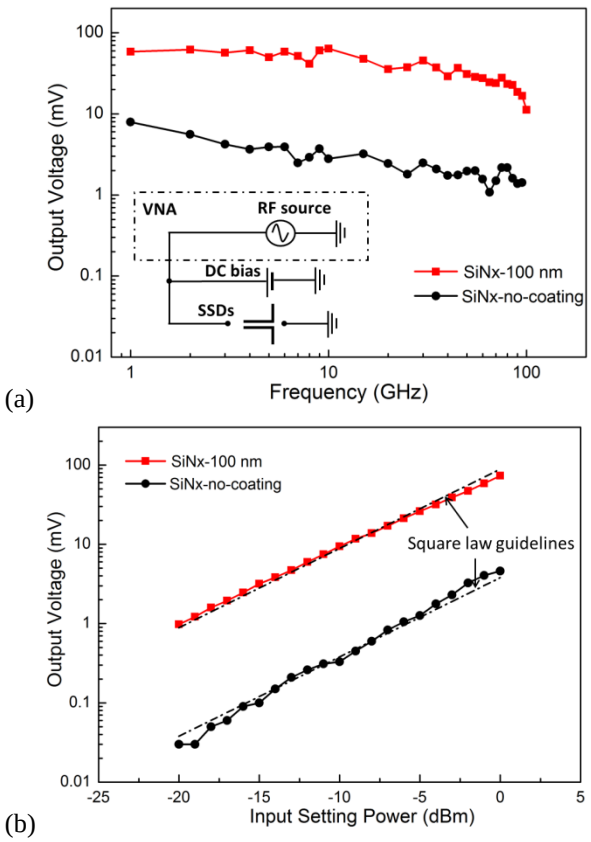

Figure 3. (a) Comparison of RF performance of SiN_x-100 nm and SiN_x-no-coating up to 100 GHz with an input power of -5.5 dBm at zero bias, and schematic representation of the RF measurement setup. (b) Output voltage as a function of input power for both devices measured at zero bias and 50 GHz.

3.3 Low-frequency Noise Measurement

The low-frequency noise performance of the devices was characterized by using a two-channel cross-correlation measurement [30, 31], as depicted in Figure 4(a). The two-channel cross-correlation method reduces the uncorrelated noise, but it cannot get rid of the input equivalent current noise of an operational amplifier (op-amp), which is mixed with the device noise in the noise measurement [30]. A low noise op-amp, TL1169, was then used to amplify the input noise signal due to its low input current noise of 1 $fA/Hz^{1/2}$ [32]. The highest frequency is approximately 10 kHz, which is limited by the amplifier bandwidth. The low-frequency noise is dominated by thermal and/or flicker noise [9, 33]. The measured noise spectral plot of the SiN_x-100 nm and SiN_x-no-coating at 32.5 nA bias and zero bias current is shown in Figure 4(b). It can be observed that the voltage noise significantly decreases by a factor of more than 10 times with the SiN_x coating.

The voltage power spectral density is proportional to $1/f^{\beta}$ at a certain current bias according to Equation 1 [9, 34].

$$S_V(f) = \frac{\alpha_H}{Nf^\beta} I^2 R^2 \quad (1)$$

where I is the bias current, R is the resistance of the device under test, N is the total number of carriers in the SSD array, f is the frequency and α_H is the Hooge's constant. The constant β is 0.96 by fitting the curve in Figure 4(b), which means the low frequency noise is dominated by *1/f* noise. The dependence between the voltage noise, $\sqrt{S_V(f)}$, and the bias current at frequency of 100 Hz is shown in Figure 4(c). The voltage noise increases linearly as the bias current enlarges then the increase slows down. The linear dependency can be explained by Hooge's empirical equation, indicating that the low frequency noise is caused by the carrier mobility fluctuation [35]. At relatively high current bias, the effective channel width could increase slightly, leading to the slight decrease of the slope in Figure 4(c) according to Equation 2, which is expressed as

$$S_V(f) = \frac{1}{M^3} \frac{1}{n^3 q^2 \mu_n{}^2} \frac{L}{W_{eff}{}^3} \frac{\alpha_H}{f^\beta} I^2 \quad (2)$$

where n is the electron concentration, M is the number of SSDs in parallel, L is the channel length of the SSD, q is the electron charge, and μ_n is the 2DEG electron mobility and W_{eff} is the effective channel width, which is 215 nm in this paper.

(a)

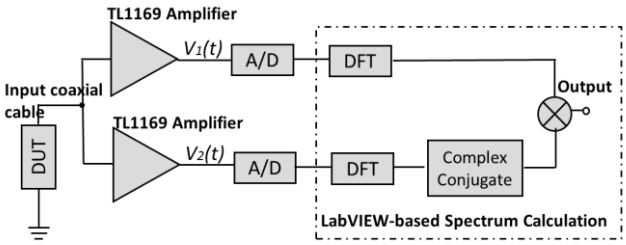

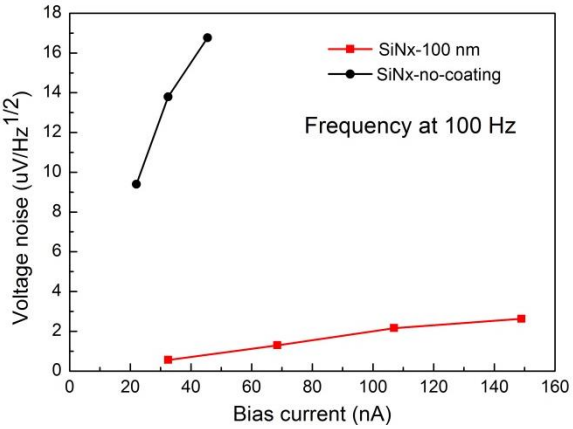

(b)

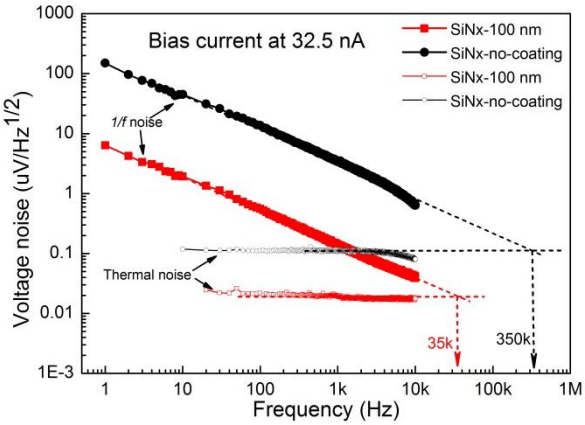

(c)

Figure 4. (a) Schematic system set-up of the two-channel cross-correlation measurement. (b) Voltage noise of device SiN_x-100 nm and SiN_x-no-coating at 32.5 nA and zero bias at room temperature with determination of the corner frequencies. (c) The linear dependence of voltage noise on the bias current at 100 Hz.

For the devices SiN_x-100 nm and SiN_x-no-coating, the channel length is 3 μm, and the zero-bias resistance is 33.3 and 616 kΩ, respectively. The device without coating has a Hooge's constant of 3.7×10^{-3}, which is lower than that of the device with coating (5.1×10^{-2}). Although the Hooge's constant of the device SiN_x-100 nm is larger, the significant reduction of the its resistance results in the reduced overall noise. In this case, *1/f* noise is caused by the scattering-induced carrier mobility fluctuations [36, 37]. The deposition of SiN_x may introduce more traps at the interface in contact with the semiconductor. The increased interface states may cause more scattering, such as lattice scattering [38] and Coulomb scattering [39], resulting in a higher Hooge's constant. Using thermal evaporation may be able to decrease the traps and surface states caused by the PECVD coating process [40]. The corner frequency, shown as the cross point of the flick noise and thermal noise in Figure 4(a), which is 35 and 350 kHz for the device SiN_x-100 nm and SiN_x-no-coating at 32.5 nA bias current, respectively. This indicates that SiN_x coating effectively suppresses the voltage noise and, thus, reduces the corner frequency. When the detected signal is smaller, the corner frequency could be further reduced for chopping [9]. NEP is another important metric of the sensitivity. When the frequency is above the corner frequency, thermal noise dominates the noise spectrum. Then the NEP is determined by thermal noise which is proportional to the resistance of SSDs. It is found that the extrinsic NEP significantly decreased by two orders of magnitude from 1.6×10^{-8} to 1.8×10^{-10} W/Hz$^{1/2}$ after SiN_x coating. The NEP can be further reduced by integrating more SSDs due to the lower total resistance as well as the thermal noise. The responsivity and NEP of the 11 SSDs in parallel

are 110 V/W at 50 GHz and 180 pW/Hz$^{1/2}$ which are comparable to results achieved by integrating thousands of SSDs on an InGaAs/InAlAs 2DEG wafer [9].

4. Conclusion

We proposed to use SiN_x coating to improve the detection properties of the nano-rectifier, i.e. SSD. SSD arrays with nano-trenches coated with and without SiN_x were fabricated, characterized, and compared. Those coated achieved high responsivity and low noise, agreeing with reported simulation results. They exhibit enhanced nonlinearity and output current, the parameters desired for room temperature THz detectors. This improvement is due to electric field coupling over the trenches causing an increase in the accumulated charges for the field effect. High-frequency measurement from 45 MHz to 100 GHz was carried out, which reveals a consistent improvement of the responsivity. The reduced low frequency noise, corner frequency and NEP demonstrate a good passivation of high-k SiN_x for the SSDs.

Acknowledgements

The authors wish to acknowledge the National Key Research and Development Program of China (Grant Nos. 2016YFA0301200 and 2016YFA0201800), the European Commission through the FP7 ROOTHz project under Grant Agreement No. 243845, the National Natural Science Foundation of China (Grant Nos. 61701283 and 11404115), Engineering and Physical Sciences Research Council (EPSRC) (Grant No. EP/N021258/1), China Postdoctoral Science Foundation funded project (Grant Nos. 2018T110689, 2017M622201, and 2016M590634), the Key Research and Development Program of Shandong Province (Grant Nos. 2017GGX10121 and 2017GGX10111), Postdoctoral Innovation Program of Shandong Province (Grant No. 20171006), Suzhou Planning Projects of Science and Technology (Grant No. SYG201616), and the Fundamental Research Funds of Shandong University (Grant No. 2016WLJH44) for supporting this work.

References

[1] Ferguson B and Zhang X-C 2002 Materials for terahertz science and technology *Nat. Mater.* **1** 26-33

[2] Balocco C *et al.* 2005 Microwave detection at 110 GHz by nanowires with broken symmetry *Nano Lett.* **5** 1423-1427

[3] Song A M, Missous M, Omling P, Peaker A R, Samuelson L, and Seifert W 2003 Unidirectional electron flow in a nanometer-scale semiconductor channel: A self-switching device *Appl. Phys. Lett.* **83** 1881-1883

[4] Balocco C, Kasjoo S R, Lu X F, Zhang L Q, Alimi Y, Winnerl S, and Song A M 2011 Room-temperature operation of a unipolar nanodiode at terahertz frequencies *Appl. Phys. Lett.* **98** 223501

[5] Balocco C *et al.* 2008 THz operation of asymmetric-nanochannel devices *J. Phys.: Condens. Matter* **20** 384203

[6] Westlund A, Sangare P, Ducournau G, Nilsson P-A, Gaquiere C, Desplanque L, Wallart X, and Grahn J 2013 Terahertz detection in zero-bias InAs self-switching diodes at room temperature *Appl. Phys. Lett.* **103** 133504

[7] Sangare P *et al.* 2013 Experimental demonstration of direct terahertz detection at room-temperature in AlGaN/GaN asymmetric nanochannels *J. Appl. Phys.* **113** 034305

[8] Al-Dirini F, Skafidas, E and Nirmalathas, A 2013 Graphene self switching diodes with high rectification ratios *13th IEEE International Conference on Nanotechnology*

[9] Balocco C, Kasjoo S R, Zhang L Q, Alimi Y, and Song A M 2011 Low-frequency noise of unipolar nanorectifiers *Appl. Phys. Lett.* **99** 113511

[10] Westlund A *et al.* 2014 On the effect of δ-doping in self-switching diodes *Appl. Phys. Lett.* **105** 093505

[11] Millithaler J F, Iñiguez-de-la-Torre I, González T, Mateos J, Sangaré P, Ducournau G, and Gaquière C 2013 Noise in terahertz detectors based on semiconductor nanochannels *22nd International Conference on Noise and Fluctuations (ICNF)*

[12] Iñiguez-De-La-Torre I, Rodilla H, Mateos J, Pardo D, Song M, and Gonzlez T 2009 Terahertz tunable detection in self-switching diodes based on high mobility semiconductors: InGaAs, InAs and InSb *J. Phys: Conf. Ser.*

[13] Westlund A *et al.* 2015 Optimization and small-signal modeling of zero-bias InAs self-switching diode detectors *Solid-State Electron.* **104** 79-85

[14] Zakaria N F, Kasjoo S R, Zailan Z, Isa M M, Taking S, and Arshad M K M 2017 Permittivity and temperature effects on rectification performance of self-switching diodes with different geometrical structures using two-dimensional device simulator *Solid-State Electron.* **138** 16-23

[15] Farhi G, Morris D, Charlebois S A, and Raskin J P 2011 The impact of etched trenches geometry and dielectric material on the electrical behaviour of silicon-on-insulator self-switching diodes *Nanotechnology* **22** 435203

[16] Iñiguez-De-La-Torre I, Mateos J, Pardo D, Song A M, and González T 2009 Noise and terahertz rectification linked by geometry in planar asymmetric nanodiodes *Appl. Phys. Lett.* **94** 093512

[17] Iniguez-de-la-Torre I, Mateos J, Pardo D, Song A M, and Gonzá lez T 2010 Enhanced Terahertz detection in self-switching diodes *Int. J. Numer. Model. Electron. Networks Devices Fields* **23** 301-314

[18] Frank M M, Kim S, Brown S L, Bruley J, Copel M, Hopstaken M, Chudzik M, and Narayanan V 2009 Scaling the MOSFET gate dielectric: From high-k to higher-k? *Microelectron. Eng.* **86** 1603-1608

[19] P. K. Saikia U J M, P. Saikia, B. Baishya, R Sarma and D. Saikia, 2012 Low threshold voltage pentacene OTFTs with La_2O_3 gate insulating layer using TSD *Chiang Mai Journal of Science* **39** 263-269

[20] Kauerauf T, Govoreanu B, Degraeve R, Groeseneken G, and Maes H 2005 Scaling CMOS: Finding the gate stack with the lowest leakage current *Solid-State Electron.* **49** 695-701

[21] Kaushal V, Íñiguez-De-La-Torre I, Gonzalez T, Mateos J, Lee B, Misra V, and Margala M 2012 Effects of a high-k dielectric on the performance of III-V ballistic deflection transistors *IEEE Electron Device Lett.* **33** 1120-1122

[22] Hurley P K *et al.* 2008 Interface Defects in HfO_2, $LaSiO_x$, and Gd_2O_3 High-k/Metal–Gate Structures on Silicon *J. Electrochem. Soc.* **155** 8

[23] Yeo Y-C, King T-J, and Hu C 2003 MOSFET Gate Leakage Modeling and Selection Guide for Alternative Gate

Dielectrics Based on Leakage Considerations *IEEE Trans. Electron Devices* **50** 9

[24] Pey K L, Ranjan R, Tung C H, Tang L J, Lo V L, Lim K S, Selvarajoo T A L, and Ang D S 2005 Breakdowns in high-k gate stacks of nano-scale CMOS devices *Microelectron. Eng.* **80** 353-361

[25] Lukyanchikova N, Garbar N, Kudina V, Smolanka A, Put S, Claeys C, and Simoen E 2009 On the 1/f noise of triple-gate field-effect transistors with high-k gate dielectric *Appl. Phys. Lett.* **95** 032101

[26] Xu K-Y, Wang G, and Song A 2007 Electron transport in self-switching nano-diodes *J. Comput. Electron.* **6** 59-62

[27] Kim H, Thompson R M, Tilak V, Prunty T R, Shealy J R, and Eastman L F 2003 Effects of SiN passivation and high-electric field on AlGaN-GaN HFET degradation *IEEE Electron Device Lett.* **24** 421-423

[28] Sung-Woon M, Jongsub L, Deokwon S, Sungdal J, Hong Goo C, Heejae S, Jeong Soon Y, John T, and Sungwon D R 2014 High-voltage GaN-on-Si hetero-junction FETs with reduced leakage and current collapse effects using SiN_x surface passivation layer deposited by low pressure CVD *Jpn. J. Appl. Phys.* **53** 08NH02

[29] Iliescu C, Tay F E H, and Wei J 2006 Low stress PECVD-SiN_x layers at high deposition rates using high power and high frequency for MEMS applications *J. Micromech. Microeng.* **16** 869-874

[30] Sampietro M, Fasoli L, and Ferrari G 1999 Spectrum analyzer with noise reduction by cross-correlation technique on two channels *Rev. Sci. Instrum.* **70** 2520-2525

[31] Crupi F, Giusi G, and Pace C 2007 Two-channel amplifier for high-sensitivity voltage noise measurements *IEEE Instrumentation and Measurement Technology Conference Proceedings (IMTC)*

[32] Manfredi P F, Speziali V, and Svelto F 1994 Extremely low-noise amplifier for interfacing active devices to instruments for spectral analysis *Rev. Sci. Instrum.* **65** 3848-3852

[33] Duran H C, Ren L, Beck M, Py M A, Ilegems M, and Bachtold W 1997 Low frequency noise in dry and wet etched InAlAs/InGaAs HEMTs *IEEE International Symposium on Compound Semiconductors*

[34] van der Ziel A 1988 Unified presentation of 1/f noise in electron devices: fundamental 1/f noise sources *Proc. IEEE* **76** 233-258

[35] Dutta P and Horn P M 1981 Low-frequency fluctuations in solids: 1/f noise *Rev. Mod. Phys.* **53** 497-516

[36] Ghibaudo G, Roux O, Nguyen-Duc C, Balestra F, and Brini J 1991 Improved analysis of low frequency noise in field-effect MOS transistors *Phys. Status Solidi A* **124** 11

[37] Hooge F N 1976 1/f Noise *Physica* **83B** 10

[38] Jindal R P, and Ziel A 1981 Model for mobility fluctuation 1/f noise *Appl. Phys. Lett.* **38** 290-291

[39] Shahriar Rahman M, Morshed T, Devireddy S P, Celik-Butler Z, Quevedo-Lopez M A, Shanware A, and Colombo L 2008 Effect of nitrogen incorporation on 1/f noise performance of metal-oxide-semiconductor field effect transistors with HfSiON dielectric *J. Appl. Phys.* **103** 033706

[40] Zhu G, Wang H, Yiming W, Feng X, and Song A 2016 Performance enhancement of AlGaN/AlN/GaN high electron mobility transistors by thermally evaporated SiO passivation *Appl. Phys. Lett* **109** 113503